Dynamic Energy Grouping in Multigroup Radiation Transport Calculations

Nick Whiting
Bloomfield High School

Advisor: Dr. Reuben Epstein

University of Rochester
Laboratory for Laser Energetics
2006 Summer High School Research Program

Abstract

During an OMEGA inertial confinement fusion (ICF) implosion, some of the absorbed laser energy is reemitted by the shell of the target as thermal radiation. In order to simulate the radiative heating of the core of the target and other radiative effects, numerical models of radiation transport are included in ICF simulation codes. These models typically divide the radiation spectrum into many energy groups. Unfortunately, these simulations can take a long time to run if the radiation transport calculation is repeated for each of a large number (e.g. 40) of energy groups. A new strategy for reducing the number of groups has been evaluated using a simple radiation program. A common technique for reducing the time needed for the radiation simulation is to regroup a large number of energy groups into fewer, larger groups in a way that avoids too great a loss of precision. The novel feature of the new strategy is adjust the boundaries of these few energy groups automatically at regular time intervals, each time optimizing the resolution of the spectrum, thus improving the accuracy of the calculations without significantly lengthening the processing time. My program, based on an earlier version by Brian MacPherson,[1] has been used to develop and analyze this method for radiation transport test cases. I will show results demonstrating this method and how it can compensate for the inaccuracies due to the reduced spectral resolution of four-group calculations.

1-Introduction

The numerical simulation of hydrodynamics is very important at the Laboratory for Laser Energetics in designing ICF experiments and in testing our understanding of the outcomes of these experiments. At the moment, these simulations may take hours, or even days, to complete. This long simulation time stems from the complexity and number of the arithmetic operations that must be completed to simulate the hydrodynamics of laser-driven implosions, including the transport of radiation through the target material. These calculations involve collecting all possible photon energies ($h\nu$) into some number of intervals or "groups," and perform the transport calculation on each of these groups. This number of groups is usually 48, 12, or 4 in the simulations used at LLE. The accuracy and time required for calculation are directly related to each other. The time required in this simulation can be reduced by regrouping those photon energy groups into a smaller number of groups.

This project worked with a model problem in which a 1 keV blackbody spectrum was incident on a planar slab of material. The time evolution of the temperature profile in the slab, which depends on radiation transport in the slab, was calculated. In the case of the program I worked with, we chose to use 40 intervals and 4 regrouped intervals of photon energy, which cut the time required to simulate the radiation transport by a significant amount (ideally, a factor of 10). Unfortunately, this time-saving measure loses accuracy when compared with its many-group counterpart due to the relative lack of spectral resolution. A proposed remedy for this inaccuracy is "dynamic regrouping," in which this regrouping is repeated periodically over the course of the simulation so that the boundaries of the four energy groups change, adapting to the radiation spectral energy density at any given point in time. If this method works as intended, it would retain the time-efficiency of static regrouping while retaining much of the accuracy of the many-group calculations. In order to test this method, a program was written in 2005 by Brian MacPherson.[1] This program only took the method as far as "static regrouping," where the same 4 groups are kept fixed throughout the calculation. I wrote a dynamic regrouping section of code into this program. I also addressed a number of problems associated with the length of the time steps, the calculation of the new groupings, and various other sections of the program. I processed my results using the PV Wave

Advantage programming environment.[2]

2-Method

2.1 Radiation Transport

In simulating radiation transport and demonstrating dynamic regrouping, the program must calculate numerous properties and radiative effects experienced by the material. The most important quantities are opacity κ_ν, emissivity ε_ν, intensity I_ν, radiation spectral energy density U_ν, and matter temperature T. All energy quantities, such as kT and hν are expressed in units of keV.

2.1.1 Opacity

Opacity is the material property that determines the rate at which the material absorbs radiation. This may be dependent on a number of properties, such as the temperature, density, and composition of the material, and also on the frequency (or photon energy) of the incident radiation. In my program, I used simple opacity expressions chosen by Fleck and Cummings[3] for their standard test problems. The opacity κ_ν is equal to:

$$\kappa_\nu = \frac{27(1-e^{-h\nu/kT})}{[h\nu(keV)]^3} cm^{-1}, \tag{1}$$

where $(1-e^{-h\nu/kT})$ is a correction for stimulated emission. The subscript ν denotes photon frequency or energy dependence. In this equation, the opacity is inversely related to the cube of the photon energy, so higher-energy photons will penetrate farther into the slab. This opacity is not strongly temperature dependent, but I did work with a strongly temperature dependent opacity at one point,

$$\kappa_\nu = \frac{27(1-e^{-h\nu/kT})}{[h\nu(keV)]^3[kT(keV)]} cm^{-1}, \tag{2}$$

Here, the opacity is also inversely related to temperature kT. This program and these opacity expressions are needed only for the analysis of the dynamic regrouping method, and more complicated and quantitatively accurate representations of real material

opacities are not required.

2.1.2 Emissivity

Emissivity is the rate at which a material emits radiation. This rate is determined by the properties of the material (temperature, composition, and density). For my program, Kirchoff's law was used for the calculation of emissivity:

$$\varepsilon_\nu = \kappa_\nu B_\nu(T). \tag{3}$$

This equation relates emissivity ε_ν directly to opacity κ_ν by the Planck function of temperature $B_\nu(T)$. In this program, the Planck function is:

$$B_\nu(T) = 4\pi \frac{5.04\times10^{22}\left[h\nu(keV)\right]^3}{(e^{h\nu/kT}-1)} \frac{erg}{cm^2 keV\,\sec}. \tag{4}$$

2.1.3 Intensity

As radiation travels through the slab, it is both absorbed and emitted. This produces an intensity I_ν of radiation, given by the equation of radiative transfer, where dI_ν/ds, the rate of change of I_ν with distance s along the propagation path, is:

$$\frac{dI_\nu}{ds} = \frac{\varepsilon_\nu}{4\pi} - \kappa_\nu I_\nu. \tag{5}$$

In its calculation of intensity, the program uses the solution to Eq.5 giving the intensity at any given distance s and for any given photon energy hν. The solution for a slab of uniform opacity κ_ν and emissivity ε_ν for the intensity $I_\nu(s)$ along a straight line path starting from s=0, where $I_\nu(0) = I_{\nu 0}$ is

$$I_\nu(s) = \frac{\varepsilon_\nu}{4\pi\kappa_\nu} + \left(I_{\nu 0} - \frac{\varepsilon_\nu}{4\pi\kappa_\nu}\right)e^{-\kappa_\nu s}. \tag{6}$$

2.1.4 Radiation Energy Density

The radiation spectral energy density is the spatial density of radiation energy within a unit range of photon energy at some distance s into the slab. The

radiation spectral energy density is given by:

$$U_\nu(s) = 2\pi \int_{-1}^{1} I_\nu(s) d(\cos\theta). \tag{7}$$

In this equation, the intensity values are integrated over all path angles θ, where θ specifies the photon path direction relative to the slab normal direction θ = 0. This is to account for radiation being emitted in all directions. The intensity is independent of the azimuthal angle ϕ due to the planar symmetry of the problem. In calculating the intensity over the full 180° range of θ, the program splits 180° into 16 segments of equal solid angle. The radiation energy density is of particular importance in calculating and understanding the matter temperature results.

2.1.5 Matter Temperature

The evolution of the matter temperature is dependent on the rate of energy absorption determined by the opacity κ_ν, the cooling rate determined by the emissivity ε_ν, and the intensity I_ν of the radiation at that distance into the slab:

$$C_V \frac{dT}{dt} = \int\int \kappa_\nu I_\nu d\Omega d(h\nu) - \int \varepsilon_\nu d(h\nu). \tag{8}$$

Here, C_V is the specific heat of the material that is being simulated. In the test problems, it is a constant set to $C_V = 0.5917 a T_0^{\,3}$, where a is the radiation energy density constant, $a = 1.37 \times 10^{14} \frac{erg}{cm^3 keV^4}$. The matter temperature equation gives two important terms: the absorption rate and the emission rate. The absorption rate is given by the opacity multiplied by the intensity $\kappa_\nu I_\nu$ integrated over all angles $\int d\Omega = 2\pi \int d(\cos\theta)$ and over all photon energy values $\int d(h\nu)$. The emission rate is the emissivity of the material ε_ν integrated over all photon energy values hν. These values are used to find the matter temperature after a finite time step Δt:

$$T = \frac{T_0 \left[C_V T_0 + \int\int \kappa_\nu I_\nu d\Omega d(h\nu) \Delta t + (\alpha - 1) \int \varepsilon_\nu d(h\nu) \Delta t \right]}{C_V T_0 + \alpha \int \varepsilon_\nu d(h\nu) \Delta t}. \tag{9}$$

Eq.9 expresses the temperature T at the end of the time step as an "explicit," "implicit," or intermediate solution of Eq.8, depending on the value of the parameter α being 0, 1, or an intermediate value.[3] When Eq.8 is solved explicitly ($\alpha = 0$) for T, the T-dependent terms on the right-hand side of Eq.8 are first written entirely in terms of the initial T value, T_0. The implicit solution ($\alpha = 1$) is the opposite, in the sense that the right-hand side of Eq.8 is first written in terms of the final value of T, which is T itself. The implicit formulation of Eq.8, expressed as Eq.9 with $\alpha = 1$, is used by the program to determine the matter temperature.

2.2 Existing Simulation

At the Laboratory for Laser Energetics, two main hydrocodes are used. These are the DRACO (2D hydrodynamics modeling) and LILAC (1D hydrodynamics modeling) codes. These codes can calculate radiation transport by grouping all photon energy values into a relatively large number of groups in order to preserve accuracy. This entails a large number of calculations and is extremely time consuming. In handling the angle-dependent aspect of radiation transport, the hydrocodes almost always use the diffusion approximation, a more approximate method than we used in this program. Some effort has been taken to shorten the time needed for these simulations to run by gathering photon energy values into a smaller number of groups, but no automated dynamic regrouping strategy has yet been implemented. These simulations are needed for the researchers at the lab to simulate ICF implosions in order to better design experiments. Reducing the amount of time necessary to run a simulation without losing a significant amount of precision would prove extremely valuable to the researchers at the LLE.

2.3 Static Regrouping

Static regrouping was implemented by consolidating a large number of small groups into a smaller number of larger groups that remain fixed throughout the calculation. In my work, I used a test problem of Fleck and Cummings where a 4 cm-thick slab is irradiated by a 1-keV blackbody spectrum. Figure 1 is a contour plot of the spectral energy density of the slab of material at 50 ps (20 time steps). This is the point at which the photon energy groups are first recalculated. Before this, the values are collected into 40 photon energy groups, each of which was 0.25 keV wide. Then, these

groups are regrouped into 4 groups. The boundaries of these new groups are shown in Fig. 1 as horizontal lines. After this, the calculation continues, using only these 4 groups. An inaccuracy in the spectral energy density is caused by the relatively poor spectral resolution resulting from using only 4 groups. The inaccuracy produced by the regrouping remains throughout the course of the calculation and builds upon itself. The time at which the many-group calculation is converted to the few-group calculation also has a significant impact on the accuracy of the calculation. Also, the program represents conditions at a finite number of distances into the slab. The slab is divided into 10 finite distance intervals, as is done in the Fleck-Cummings test problems,[3] giving only quantities defined at ten spatial points throughout the slab. The program uses finite difference integrations in time, distance, angle, and energy to handle these calculations.

2.4 Dynamic Regrouping

Dynamic regrouping was suggested[4,1] as a possible solution to the difficulties presented by static regrouping. This method involves the successive recalculation of the boundaries of the four large groups at regular time intervals. This regrouping is repeated periodically using spectral energy density values calculated with the same 40 groups used in determining where the boundaries of the four large groups were to be placed in the first regrouping. The simulation then continues for the following predetermined cycling time interval using only the four new groups. Once the cycling time has expired, the simulation goes on to perform yet another 40-group time step to produce a smooth spectrum with a smoothness similar to that of the spectral energy density shown earlier in Fig. 1. Then, a new set of 4-group boundaries is obtained from the smooth 40-group spectral energy density, and the program cycles again. All of this is done automatically by the program. Overall, this method of simulation improves upon the approximation of a low-resolution 4-group spectral grid without adding a significant amount of calculation time.

The contour plots of radiation spectral energy density produced during the simulation provide a good illustration of dynamic regrouping. Originally, the spectral energy density is smooth and accurate (Fig. 1). The contours of the 4-group spectrum can be seen from the contour plots produced during the 4-group calculations, such as Fig. 2 and Fig. 3. These spectra are seen to be very approximate, due to the relatively poor

spectral resolution, compared with the smoothness of the spectra produced early in the simulation. Figure 4 is an example of a spectral energy density produced from a 40-group calculation later in the simulation (447.5 ps). This plot illustrates the point in the dynamic regrouping cycle when the simulation returns to a more accurate representation of the spectral energy density for one time step in order to allow new group boundaries to be obtained for the 4-group time steps to be done next. This is the key detail in the dynamic regouping cycle.

2.5 The Program

Dynamic regrouping has been incorporated into the radiation transfer program originally written by Brian MacPherson.[1] This program consists primarily of a time-stepping loop where the length of the time step is controlled. In each time step, the opacity and the emissivity are calculated for each of the 10 slab spatial zones. Then, the program obtains the intensity by numerically integrating Eq.5 and then uses Eq.7 to obtain the radiation energy density. The program goes on to calculate the change in matter temperature with Eq.9, which is the solution to Eq.8. At the regrouping time, new boundaries are calculated for the four large energy groups. Then, the program repeats this process in the next regrouping cycle.

2.5.1 Opacity and Emissivity Calculations

The program uses Eq.1 and Eq.3 to calculate the opacity and emissivity, respectively. Equation 2 was also used as an alternative temperature-dependent opacity in another Fleck-Cummings test problem.[3] The opacity and emissivity functions are evaluated at each increment of distance into the material and at each of the 40 photon energy values. These stored values are used later in the calculation of intensity and in the calculation of the matter temperature. The emissivity and opacity are recalculated at every time step.

2.5.2 Intensity and Radiation Energy Density

The program first calculates the intensity values at all distances s along each of the 8 paths spaced equally in solid-angle intervals from 0° to 90°, relative to the forward direction (θ=0°), away from the blackbody source, and for each photon energy value.

These integrations are initialized with $I_{\nu 0}$ equal to the blackbody spectrum at T = 1 keV. The program uses Eq.6 to perform the integration along s. The final intensity at the end of each distance increment is used to evaluate the contribution to the absorption rate term in Eq.9 for each distance step, for each photon energy, and for each angle. This calculation is also performed in an identical fashion for the intensities along the remaining 8 paths from 90° to 180°, except that each of these rays are initialized with $I_{\nu 0} = 0$ at the outer boundary. All these values of intensity are then used to determine the radiation spectral energy density using Eq.7. These values of radiation energy density can then be displayed in contour plots so that the radiation energy density can be compared at different points in time. Figure 1 and Fig. 4 show plots of radiation energy density at two different points in time. It can be seen that early in the simulation, higher energy photons penetrate deeper into the material, but that later in the simulation the distribution of low and high energy photons deep in the material is more even.

2.5.3 Matter Temperature

The matter temperature evolution is obtained from Eq.8 after calculating the radiation absorption and emission rates. The opacity is multiplied by intensity and integrated over all angles and all photon energies to give the absorption rate. The emissivity is integrated over all photon energies to give the emission rate. The absorption and emission rates are used in Eq.9 to find the matter temperature. The program solves this equation implicitly, setting α equal to 1. Figure 5 is plotted with respect to distance into the slab at one specific time (750 ps) in the simulation. Figure 6 is the temperature at one distance into the slab (1.2 cm) over the entire time that the slab is exposed to the incident 1 keV blackbody spectrum.

2.5.4 Regrouping

Regrouping is performed automatically after a certain number of time steps. This number can be set to any value, but I chose to have it perform the first regrouping after 20 time steps (50 ps), and then regroup at intervals of 40 time steps (100 ps). In the calculation of the new 4-group boundaries, the program uses the 40-group radiation spectral energy density and places one boundary at the maximum of the spectral energy density integrated over the whole volume, one boundary at each of the 50%-maximum

value points, and one boundary each at the lowest and highest photon energy values. This regrouping reduces the number of calculations performed, but it also creates radiation energy density contour plots that are more approximate due to the loss of spectral resolution.

3-Results

3.1 Dynamic Regrouping vs. Static Regrouping

In the first 60 time steps (150 ps), through the end of the first dynamic regrouping cycle, the dynamic and static regrouping results are the same, since both methods use the same 4 groups during this time. Figure 6 shows this with the 40-group calculation as a solid line, dynamic regrouping as a heavy-dotted line, and static regrouping as a light-dotted line. The dynamic regrouping result deviates from the static regrouping result after the 60^{th} time step (150 ps). Immediately after this time step, the dynamic regrouping performs a single 40-group calculation of the radiation spectral energy density to use in determining a new set of 4-group boundaries. Since these 4 new groups allow better resolution of the spectrum at this point in time, the temperature results begin to more closely follow the results of a full 40-group calculation. This improvement is very slight and is not clearly visible in Fig. 6 at this depth (1.2 cm) until after the next regrouping cycle at the 100^{th} step (250 ps). Figure 7 also illustrates these results, showing the effects of dynamic regrouping on the temperature deeper (2.7 cm) into the slab. Here, the dynamic regrouping results deviate visibly toward the 40-group results after the second regrouping at the 60^{th} time step (150 ps). This simulation also has produced temperature profiles that are similar to those that were obtained in test problems by Fleck and Cummings.[3] Figure 5 is a good example of these temperature profiles, and again shows improvement over static regrouping when dynamic regrouping is used. This improvement is probably the most important result of my work.

3.2 Time step Variation

The size of the time step also had some effect on the accuracy of both static and dynamic regrouping. If the time step was too large, the temperature profile errors at early times could be excessive, as is illustrated by the example in Fig. 8. As the time step comes closer and closer to zero, the accuracy of the results increases because the

difference equation becomes a better approximation of the differential equation. Figure 9 shows the accuracy produced by using a time step that is fairly small. Unfortunately, with a significantly smaller time step, the time required to run the program increases by a factor that is inversely related to that time step. I had to choose a time step that was small enough to produce relatively accurate results, but that did not require an especially large amount of time to compute. After experimenting with a few other values, I chose a 2.5 ps time step as the most efficient. As can be seen from Figure 10, this time step still provides improved accuracy over static regrouping, while at the same time not being too small to undo the efficiencies gained by using regrouping. With any significant change to the test-case problem (such as adding strongly temperature-dependent opacity), the size of the time step may have to be adjusted to maintain accuracy. For example, a strongly temperature-dependent opacity can greatly increase the heating rate, causing the matter temperature values to jump up to many times the 1 keV source radiation temperature if the time step is too large, which is physically impossible. In order to run the calculation for the same amount of simulated time, the number of time steps increases, and the computation time begins to become a problem once more. A different method of calculation may allow for a larger time step to be taken, but at present, the time step has a very large effect on the accuracy (and so, the usefulness) of dynamic regrouping.

3.3 Boundary Variation

In the regrouping process, boundary values for the larger energy groupings are chosen based on a calculation of the space-integrated spectral energy density. Boundaries are placed at the highest and lowest photon energy values (10.0 keV and 0.25 keV in the case of this program). A boundary is also placed at the photon energy with the highest spectral energy density. Then, two more boundaries are placed, each at the photon energies with 50% of the maximum radiation energy density. This percentage was chosen because it would distribute the energy in the groupings fairly evenly. However, I experimented with varying this percentage, and found that different percentages produced results with different accuracy. I determined this by comparing the temperature profiles produced by static and dynamic regrouping with these percentage changes to a full 40-group calculation and to the profiles produced by the default 50%

calculations (Fig.7). I raised the boundaries to 60% of the maximum, and found that static regrouping lost accuracy (Fig.11), but that dynamic regrouping regained a small amount of accuracy. I also lowered the boundaries to 40% of the maximum and found that static regrouping gained accuracy and followed dynamic regrouping more closely. Experimentation with the boundary selection strategy appears to benefit both the static and dynamic regrouping results to some degree. The boundary calculations in this regrouping strategy must be analyzed in more detail before any definite conclusions can be drawn from the results, but, at the moment, this seems to be a step in the right direction.

4-Conclusions/Future Work

In researching dynamic regrouping as an effective method for accurately and efficiently simulating radiation transfer, I have found that the dynamic regrouping retains the efficiency of static regrouping while, at the same time, more closely follows the results of a full 40-group calculation. A nearly ten-fold improvement in time efficiency was observed, as well as the improvement of accuracy, over that of static regrouping. I have also found that adjusting the regrouping method affects the accuracy of results produced by this program. By continuing to experiment with this strategy, the accuracy of dynamic regrouping may be further improved. Among the adjustable aspects are the time step length and the group boundary selection method. The time step appears to have the greatest effect on the results obtained. If it is too small, efficiency is lost, but if it is too big, accuracy is lost. The boundary calculations have a less drastic affect on the accuracy of dynamic regrouping, but they appear to have a larger effect on the accuracy of static regrouping. During further testing, this method will have to be exposed to many more test problems to determine its potential benefits or limitations. At present, dynamic regrouping has only been tested against one test problem. However, with much work remaining to be done, dynamic regrouping still appears to be a promising method of improving the efficiency of radiation transfer simulations.

5-References

[1] Brian MacPherson, “Dynamic Energy Grouping in Multigroup Radiation Transport Calculations,” 2005 Summer Research Program for High School

Juniors, Student Research Reports LLE Laboratory Report #343.

[2] PV-Wave Advantage Programming Environment

[3] J. A. Fleck, Jr. and J. D. Cummings, “An implicit Monte Carlo scheme for calculating time and frequency dependent nonlinear radiation transport,” *Journal of Computational Physics*, vol. 8, pp. 313-342, 1971.

[4] R. Epstein, private communication, Jul-Aug. 2006.

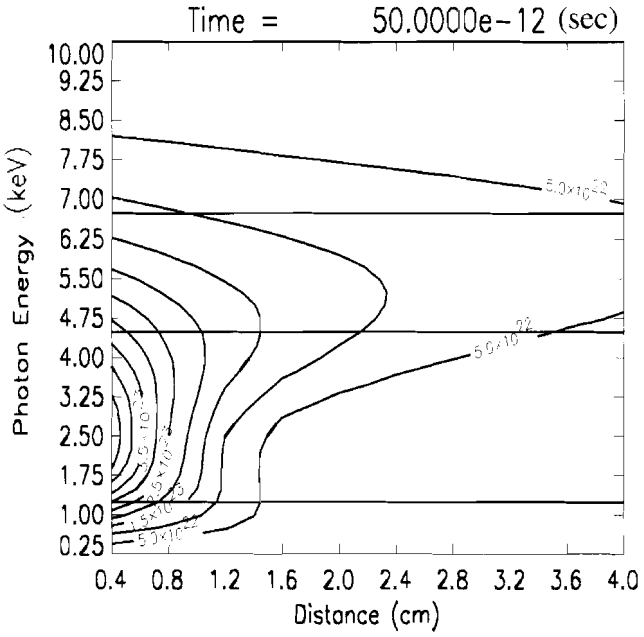

Fig.1: Contour plot of the radiation spectral energy density as a function of distance into the slab and photon energy using 40 energy groups. The boundaries selected for the 4-group calculation in Fig.2 are shown as horizontal lines.

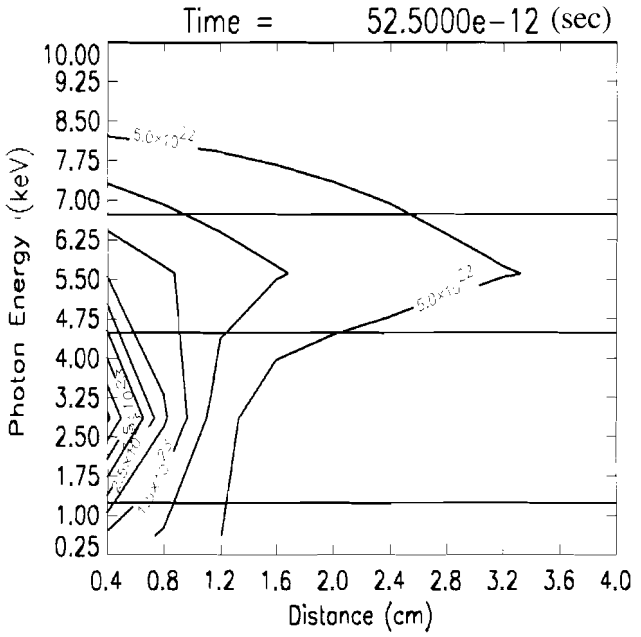

Fig.2: Same as Fig.1, except that the radiation spectral energy density is calculated using only 4 groups.

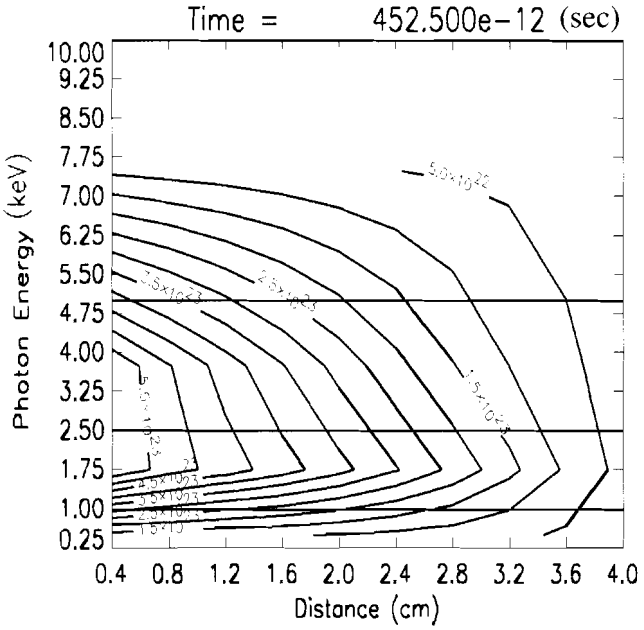

Fig.3: Same as Fig.2, but 160 time steps (400 ps) later.

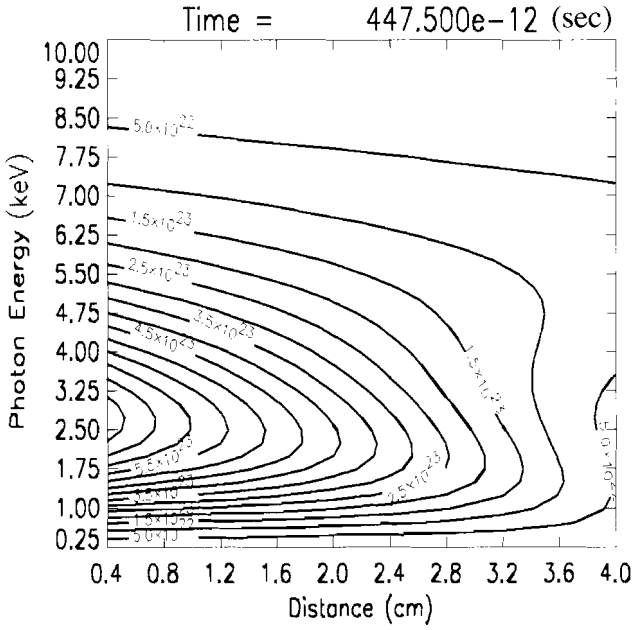

Fig.4: Same as Fig.1, but 159 time steps (397.5 ps) later when the smoother 40-group spectrum is obtained. This plot shows the deeper penetration of the lower energy photons than at earlier times in the simulation, such as is shown in Fig. 1.

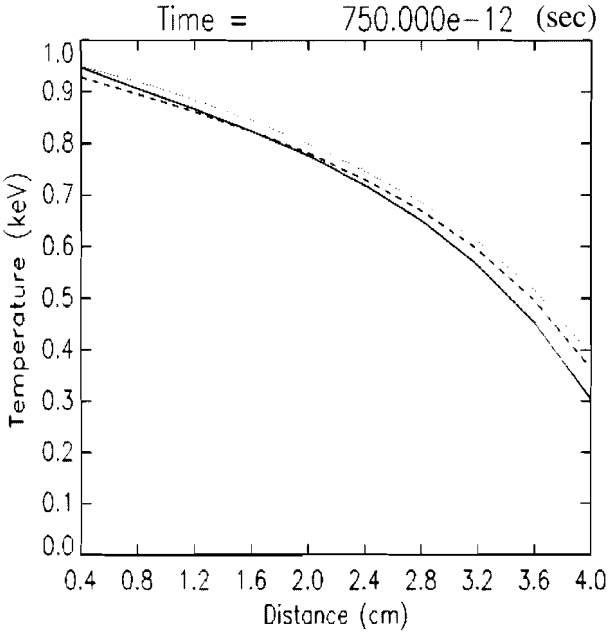

Fig.5: Matter temperature profiles similar to those produced by Fleck and Cummings.[3] A full 40-group calculation is represented by the solid line. Static regrouping is the dotted line, and dynamic regrouping is the dashed line.

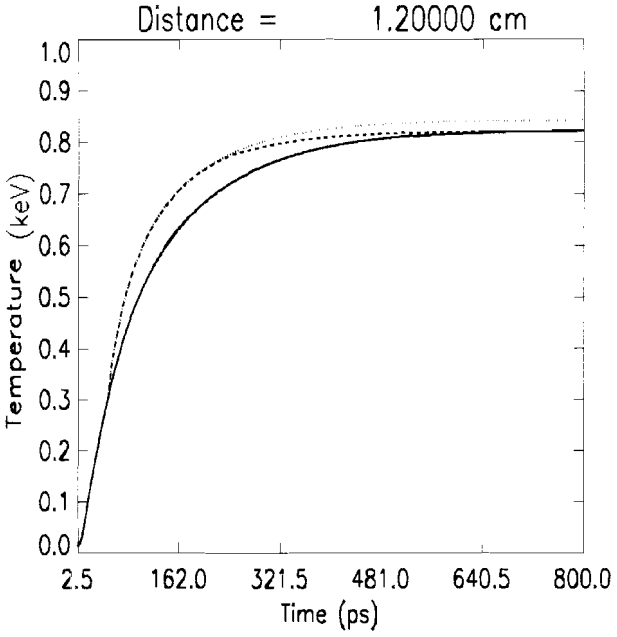

Fig.6: Matter temperature profile in a single zone (at a distance 1.2 cm) with respect to time. The solid line is a 40-group calculation, the dashed line is dynamically regrouped, and the dotted line is static regrouping.

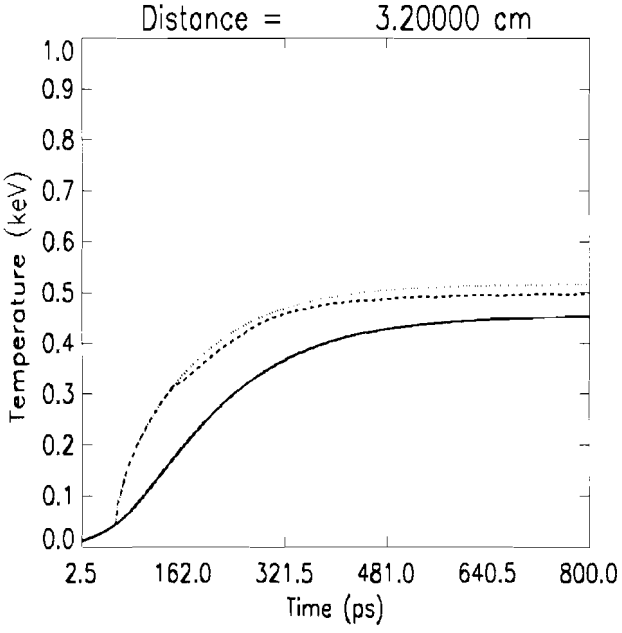

Fig.7: Same as Fig.6, but at a zone that is 3.2 cm into the slab of material. The photon energy boundaries are at 50% of the maximum photon energy density value for this calculation.

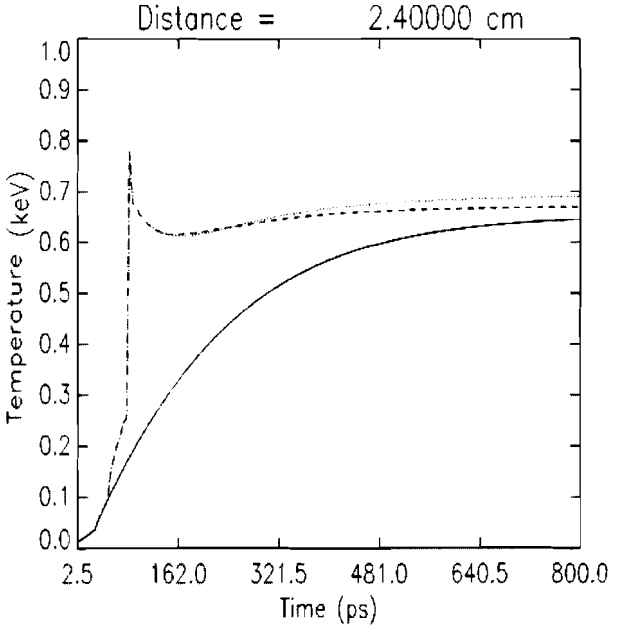

Fig.8: Same temperature history as shown in Fig.7, but at a zone 2.4 cm into the slab and calculated using a 5.0 ps time step.

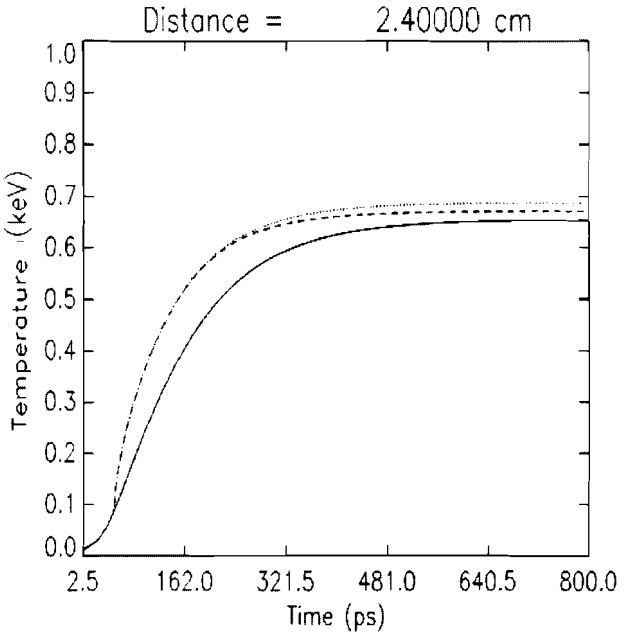

Fig.9: Same as Fig.8, but calculated with a 1.25 ps time step.

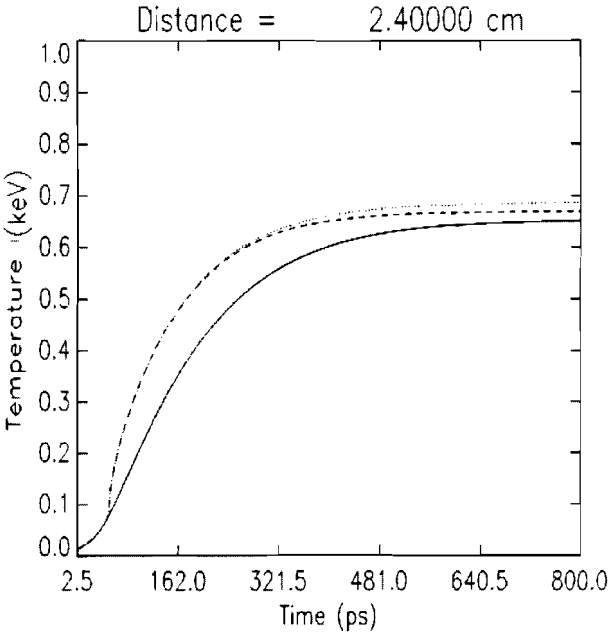

Fig.10: Same as Fig.8, but calculated using a 2.5 ps time step.

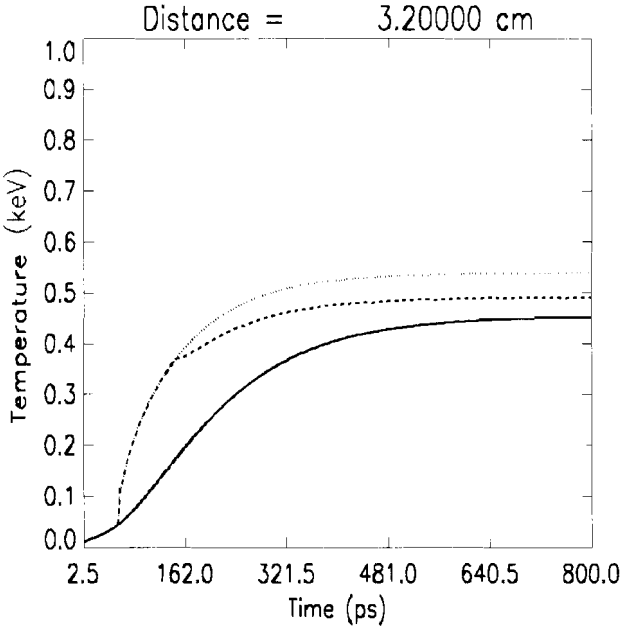

Fig.11: Same as Fig.7, except the photon energy boundaries were set at 60% of maximum photon energy density value for this calculation.

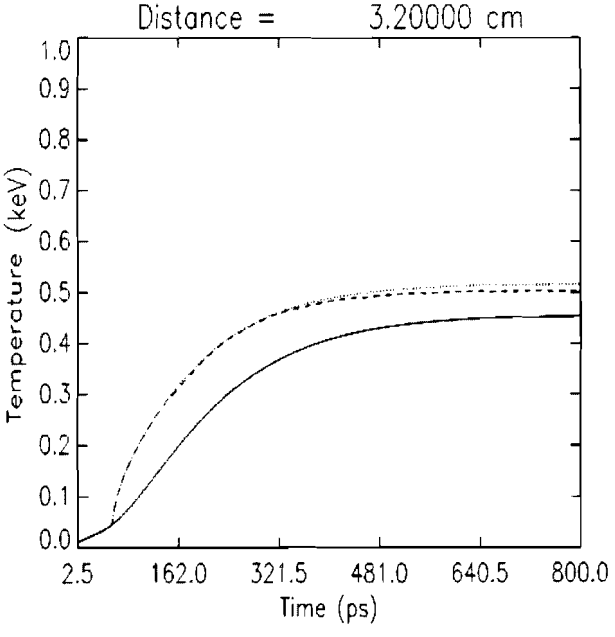

Fig.12: Same as Fig. 7, but the photon energy boundaries were set at 40% of maximum photon energy density value for this calculation.